

# Robust Power System Stabilizer Design for an Industrial Power System in Taiwan using Linear Matrix Inequality Techniques

Hung-Chi Tsai, Chia-Chi Chu, *Member, IEEE*, and Yung-Shan Chou *Member, IEEE*

**Abstract**—This work proposes the design of robust Power System Stabilizers (PSS) for the supplementary damping of the largest industrial power system in Taiwan. The design procedure integrates several existing robust control techniques, including the linear matrix inequality (LMI) framework, the mixed-sensitivity formulation and model-order reductions. The selection of weighting function for shaping the open loop control will also be considered. Nonlinear power system transient simulations incorporating with various faults are also performed to confirm the effectiveness of the proposed design. Simulation results have demonstrated that the resulting robust PSS can indeed enhance the damping of the low-frequency oscillations and improve system performance specifications in both the frequency domain and the time domain.

**Index Terms**—Damping Control, Power System Stabilizer (PSS), Robust Control, Linear Matrix Inequality.

## I. INTRODUCTION

WITH the increasing number of inter-connections and interchanges of electrical energy in power networks, power systems have recently experienced low-frequency oscillations, either unstable or poorly damped [1]. When severe disturbances occur or the power network is weakened by cascading outages of tie lines, the stability of the power system stability deteriorates. This oscillatory phenomenon has been observed in Taiwan's largest industrial power plant. Hence, special attention has been paid to designing control signals to damp out such oscillations. Power system stabilizers (PSSs) have been widely used in practical applications to enhance the damping of such system [2], [3]. The basic operating principle of PSSs is to generate an electrical torque component in phase with variations in the rotor's speed. By controlling the excitation system using an auxiliary stabilizing signal, the system can be damped to suppress oscillations of the rotor. Several methods have been adopted to design PSSs, including root locus method [4], sensitivity analysis [5], pole placement [6], and tuning the gain and the time constant of lead-lag compensators [2]. Although such design techniques are given by a practically operating point, they do not guarantee robustness under a wide range of operating conditions. The current design strategy moves toward robust control design to overcome this issues [3].

Among various techniques for designing robust controller, including LQG/LTR [7],  $H_\infty$  optimal control [8], [9], [10],

The authors are with the Department of Electrical Engineering, Chang Gung University, Tao-Yuan, Taiwan, R.O.C.. This work was supported by the National Science Council, Republic of China, under Grants NSC 90-2213-E-182-017-182-017, NSC 90-2213-E-182-018, and NSC 91-2213-E-182-016

[11], [12], and structured singular value (SSV) or  $\mu$  synthesis approach [13], [14], [15], [16], have been applied in designing PSSs. Although the resulting power system with robust PSSs is guaranteed to be stable even under severe disturbances, all of these methods depend on the Riccati equation to be solved. Riccati-based designs depend heavily on the proper selection of weighting functions for conditioning of the plant, and no clear method for selecting these weighting functions. Accordingly, time domain specifications cannot easily be obtained for practical PSS design.

Linear Matrix Inequality (LMI) techniques have recently emerged as powerful design techniques for various linear control systems [17]. The multi-objective design based on the LMI formulation has great potential in the field of power system damping control design [18], [19]. The selection of weights is very easy, as no restriction is imposed on the augmented plant. The LMI framework enables the placement of the closed poles in the specific region of the left-half plane to control the damping ratio. Additionally,  $H_\infty$  can be mixed with  $H_2$  and pole placement, improving the closed-loop behavior [20].

This work investigates the effectiveness of LMI techniques on designing a robust PSS for the largest industrial power plant in Taiwan. This design integrates many existing robust control techniques, including the LMI framework, the mixed-sensitivity formulation, and model-order reductions. The selection of the weighting functions for shaping the open loop control is also examined. The performance of the conventional PSS is compared with that of the proposed robust LMI design using the power system transient simulation package *PSS/E Ver 28.1* [21]. The results of simulation show that the robust PSSs using LMI technique can effectively damps out low-frequency oscillations under various operating conditions.

The work is organized as follows. Section II describes the studied power system. Section III provides a theoretical overview of the robust control design using LMI techniques. Section IV summaries a robust PSS design procedure. Section V draws conclusions.

## II. SYSTEM DESCRIPTIONS

Formosa Plastics Corporation proposed a project in central Taiwan in response the absence of raw petrochemical materials, and its restriction the development of downstream industries. The project involves more than 50 large-scale petrochemical plants, including a large thermal power plant, an Independent Power Plant (IPP) and many Cogeneration Power

TABLE I  
POWER FLOW DATA FOR THE STUDIED SYSTEM

From	To	Active power(P)	Reactive power(Q)
Bus2	Bus1	591.6 MW	94.2 MVAR
Bus2	Bus3	169.4 MW	14.2 MVAR
Bus3	Bus4	67 MW	33.4 MVAR
Bus5	Bus2	210 MW	28.2 MVAR

Plant (CPP). The combined output of generators is 1.8 million kW. Generated all energy has been sold to Taiwan Power Company (TPC) and incorporated into the national power grid.

Fig. 1 is a single line diagram of the studied system. The IPP contains generators GA1-GA3. The CPP includes the other generators. The external output of the studied system is connected to TPC, a state-owned utility. TPC is represented as an infinite bus. Table I and II show the power flow data and generation data for the system, respectively. Low-frequency oscillations with poor damping have been observed in this interconnected system. Hence, Formosa Plastics Corporation plans to install PSSs to improve the stability of the system.

The power flow data shows that the IPP and the CPP have almost identical power flows. Additionally, these two areas are connected by relatively weak tie lines (#1-#2). As illustrated in [22], this system can be approximated as a two-area system with a weak tie-line. Low-frequency oscillations has been recently observed. A corresponding dynamic model is used to describe such behaviors and analyze such oscillatory phenomena. For simplicity, network-reduction models are used to represent the overall power system [23], including (1) generator models, (2) control equipment models, and (3) load models. Herein this work, generators are described using two-axis detailed models [21], [22], [23]. The variable of the generator models includes (1) rotor angle  $\Delta\delta$ , (2) rotor speed  $\Delta\omega$ , (3) direct axis rotor flux linkage  $\Delta\psi_{kd}$ , (4) quadrature axis rotor flux linkage  $\Delta\psi_{kq}$ , (5) direct axis sub-transient voltage  $\Delta E'_d$ , and (6) quadrature axis sub-transient voltage  $\Delta E'_q$ . The control equipment includes (1) an exciter, (2) an turbine, (3) an governor, and (4) an PSS [22], [23]. The IEEE-SSGO governor/turbine model is used to represent each unit [21]. Each generator has its own exciter model. Table II describes this equipment. All loads are represented using constant impedance models.

Accordingly, the system state  $x$  includes the following entries  $x = [x_1, x_2, \dots, x_n]^T$  where

$$x_i = [\Delta\delta_i \ \Delta\omega_i \ \Delta\psi_{kdi} \ \Delta\psi_{kqi} \ \Delta E'_{di} \ \Delta E'_{qi} \ \Delta E'_{di} \ \Delta E'_{qi} \ \dots]^T$$

represents the  $i$ -th generator,  $i = 1, 2, \dots, N$ . Linearizing of the studied power system yields the state space representation,

$$\dot{x} = Ax + Bu, \quad y = Cx. \quad (1)$$

The system matrix  $A$  depends on the operating conditions. Variables  $y$  and  $u$  are vectors of output variables and control inputs respectively. After such algebraic manipulations, a 201th-order system is obtained and will be used to design a robust PSS.

### III. LMI-BASED CONTROLLER DESIGN

This section offers a brief overview of multi-objective design in terms of LMI. Theoretical details can be found in [17]. The design problem treated in this work is to construct an internally stable controller which satisfies  $H_\infty/H_2$

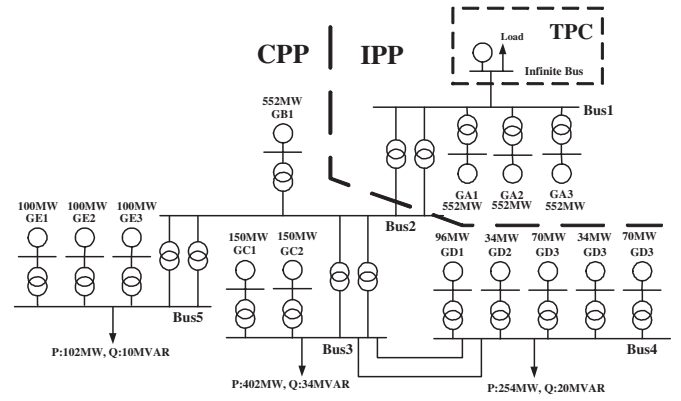


Fig. 1. The single-line diagram of an industrial power system in Taiwan.

TABLE II  
GENERATION DATA FOR THE STUDIED SYSTEM

Area	Generator	Exciter model	P (MW)	Q (MVAR)
IPP	GA1	EXPIC1	552	111
	GA2	EXPIC1	552	111
	GA3	EXPIC1	552	111
CPP	GB1	IEEET1	552	111
	GC1	IEEET1	150	21
	GC2	IEEET1	150	21
	GD1	EXAC1	25	16
	GD2	EXAC1	32	10
	GD3	EXAC1	50	15
	GD4	EXAC1	33	11
	GD5	EXAC1	47	15
	GE1	IEEET1	104	17
	GE2	IEEET1	104	17
GE3	IEEET1	104	17	

performance and pole placement. Figure 2 depicts the mixed sensitivity configuration where  $P$  indicates the open loop plant,  $K$  represents the controller to be designed.  $W_1(s)$  and  $W_2(s)$  are weighting functions for shaping characteristics of the open loop plant. The objective of the controller is to provide additional damping to the system, or equivalently to reduce the resonant peak of the closed-loop transfer function. Therefore, the state-space description of the augmented is

$$\dot{x} = Ax + B_1w + B_2u \quad (2)$$

$$z = C_1x + D_{11}w + D_{12}u \quad (3)$$

$$y = C_2x + D_{21}w. \quad (4)$$

where  $u \in R^n$  represents the control input,  $w$  is a vector of exogenous inputs (such as reference signals, disturbance signals, or sensor noise),  $y \in R^n$  represents the measured output, and  $z$  is a vector of output signals.

Let  $T_{zw}$  denotes the closed-loop transfer function from  $w$  to  $z$  for a dynamical output-feedback law  $u = Ky$

$$T_{zw} = \begin{bmatrix} W_1S \\ W_2KS \end{bmatrix}, \quad (5)$$

where  $S = (I - GK)^{-1}$  is the sensitivity function that ensures disturbance attenuation and good tracking performance.  $KS = K(I - GK)^{-1}$  handles the issues of robustness and constrains the effort of the controller. The goal of this work is to obtain a dynamic output-feedback controller under a dynamical output-feedback law  $u = Ky$ , with the following state-space representation

$$\dot{x}_k = A_k x_k + B_k y, \quad u = C_k x_k + D_k y. \quad (6)$$

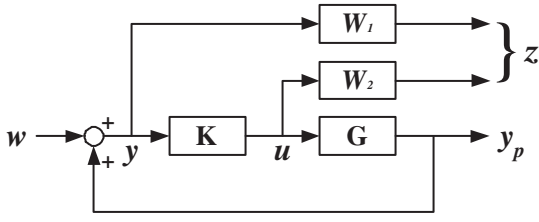


Fig. 2. Mixed Sensitivity Feedback Configuration.

The plant  $P$  and controller  $K$  are defined as above. Hence, the closed loop system can be represented

$$\dot{x}_{cl} = A_{cl}x_{cl} + B_{cl}w, \quad z = C_{cl}x_{cl} + D_{cl}w. \quad (7)$$

The  $H_\infty$ ,  $H_2$  and pole placement design objectives can be expressed as an LMI formulation, as follows.

#### A. $H_\infty$ Control

The  $H_\infty$  norm measures the system input-output gain for finite energy. Let  $\|T_{zw}\|_\infty$  denotes the  $H_\infty$  norm of  $T_{zw}$ . The objective function of  $H_\infty$  control is

$$\|T_{zw}\|_\infty = \left\| \begin{bmatrix} W_1 S \\ W_2 K S \end{bmatrix} \right\|_\infty < \gamma. \quad (8)$$

The constraint  $\|T_{zw}\|_\infty < \gamma$  can be interpreted as a disturbance rejection problem. This constraint is also useful to enforce robust stability. In the LMI formulation, the objective of  $H_\infty$  control is achieved in the sub-optimal sense if and only if there exists a symmetric matrix  $P > 0$  such that:

$$\begin{bmatrix} A_{cl}^T P + P A_{cl} & P B_{cl} & C_{cl}^T \\ B_{cl}^T P & -\gamma I & D_{cl}^T \\ C_{cl} & D_{cl} & -\gamma I \end{bmatrix} < 0. \quad (9)$$

with (8), and the  $H_\infty$  controller is said to be  $\gamma$  sub-optimal.

#### B. $H_2$ Control

Assume that  $A_{cl}$  is stable and  $D_{cl} = 0$ . The  $H_2$  norm of  $T_{zw}$  is defined by

$$\|T_{zw}\|_2^2 = \frac{1}{2\pi} \int_{-\infty}^{+\infty} \text{Tr}(T_{zw}(i\omega)^H T_{zw}(i\omega)) d\omega. \quad (10)$$

which corresponds to the asymptotic variance of the output  $z$  when the system is driven by  $w$  with white noise. The objective function of  $H_2$  control is

$$\|T_{zw}\|_2^2 = \left\| \begin{bmatrix} W_1 S \\ W_2 K S \end{bmatrix} \right\|_2^2 < \nu. \quad (11)$$

Let  $w$  be white noise. The  $H_2$  performance is useful to handle stochastic aspects such as measurement noise and random disturbances. In the LMI formulation, the  $H_2$  norm of  $T_{zw}$  does not exceed  $\nu$  when there exist two symmetric matrices  $Q > 0$  and  $P > 0$  such that:

$$\begin{bmatrix} A_{cl}^T P + P A_{cl} & P B_{cl} \\ B_{cl}^T P & -I \end{bmatrix} < 0, \quad \begin{bmatrix} P & C_{cl}^T \\ C_{cl} & Q \end{bmatrix} > 0. \quad (12)$$

where  $\text{Trace}(Q) < \nu$ ,  $D_{cl} = 0$ .

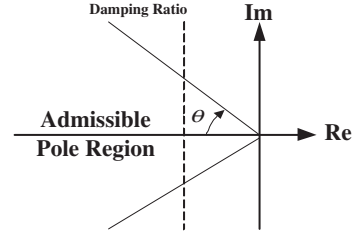


Fig. 3. LMI region

#### C. Pole Placement

The transient response of a linear system is related to the location of its poles. An acceptable transient response can be achieved by placing all closed-loop poles in a prescribed region, depicted in Fig. 3. When the closed-loop poles are in this region, it ensures minimum damping ratio  $\zeta = \cos \theta$  [17]. All of the poles of the state matrix  $A_{cl}$  inside this conical sector if and only if there exists  $P > 0$  such that:

$$\begin{bmatrix} \sin \theta (A_{cl} P + P A_{cl}^T) & \cos \theta (A_{cl} P - P A_{cl}^T) \\ \cos \theta (P A_{cl}^T - A_{cl} P) & \sin \theta (A_{cl} P + P A_{cl}^T) \end{bmatrix} < 0. \quad (13)$$

This expression can be written in Kronecker product form as

$$[W \oplus AP + W^T \oplus PA] < 0 \quad (14)$$

where

$$W = \begin{bmatrix} \sin \theta & \cos \theta \\ -\cos \theta & \sin \theta \end{bmatrix}. \quad (15)$$

#### D. Multi-Objective Controller Design

A mixed  $H_\infty/H_2$  with regional pole placement is employed in designing a robust PSS. This design problem minimize  $\nu$  and  $\gamma$  over all controllers, satisfying

$$\|T_{zw}\|_\infty < \gamma, \quad \|T_{zw}\|_2 < \nu. \quad (16)$$

The problem is a multi-objective control problem with two performance specifications. Notably, the problem of the trade-off between the  $H_\infty$  norm and the  $H_2$  norm constraint is of interest. In practice, giving up the hard constraints and proceeding as follows may be numerically advantageous. For fixed real weights  $\alpha_1$  and  $\alpha_2$ , minimize

$$\alpha_1 \|T_{zw}\|_\infty + \alpha_2 \|T_{zw}\|_2$$

over all controllers that satisfy (16). A larger  $\alpha_1$ , corresponds to a greater penalty for large values of  $\|T_{zw}\|_\infty$ , and to a stronger expectation that the optimization procedure will reduce the corresponding bound  $\gamma$ . In order to reduce calculation, This paper assumes that  $\alpha_1$  and  $\alpha_2$  are given by 1.

All inequalities in (8), (12) and (13) contain  $A_{cl}P$  which is a function of the plant  $P$  and the controller  $K$ , so the solution algorithm will involve a nonlinear formulation. Some changes of variables may simplify this nonlinear problem to a linear one. The detailed treatment is presented in [17]. In this situation, new controller variables can be obtained using the interior-point optimization algorithm [24].

#### IV. ROBUST PSS DESIGN

This section focuses on the design of a robust PSS for improving the dynamic stability of the studied system. The 201th-order linear model is used to design a robust PSS. The design procedure consists of the following steps:

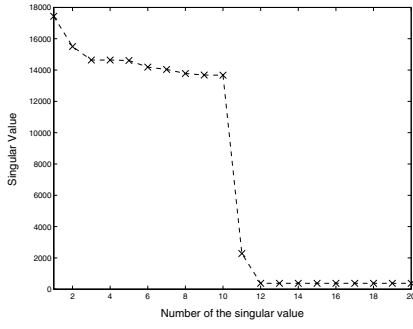


Fig. 4. Singular values of the original 201-th order power system.

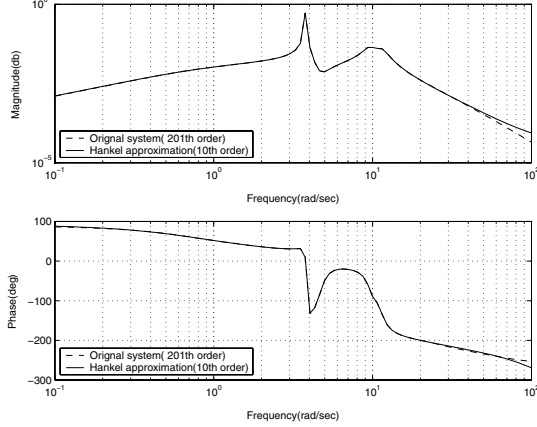


Fig. 5. Comparisons of Bode Plots: the solid line represents the original system. The dash line is 10th-order reduced system.

### A. Reducing the Plant Model

The model-order reductions of the power plant is used to reduce the computational complexity and to expedite the design process. The Hankel-norm approximation technique is used since the magnitudes of singular value can be interpreted as the strengths of each individual state. The  $\mu$ -Analysis and Synthesis Toolbox, available in Matlab [25], is used to perform this reduction. Figure 4 shows the magnitudes of the first 20 singular values of the original 201th-order plant. Since the first ten singular values are much stronger than that of the others, a 10th-order reduced system can be used to capture the essential dynamic behaviors of the original system. Figure 5 shows the Bode response of the original system and the reduced system to demonstrate that the reduced 10th-order system is very close to the full 201th-order system. Hence, this 10th-order system is used to represent the original power plant.

### B. Selecting PSS Sites

The participation factor is the sensitivity of a mode to changes in the machine's damping coefficient. It is defined by

$$\frac{\partial \lambda_i}{\partial A_{rr}} = v_{ir} u_{ir}. \quad (17)$$

$\lambda_i$  is the corresponding eigenvalue.  $A_{rr}$  is the diagonal entries of the state matrix.  $v_{ir}$ ,  $u_{ir}$  are the left eigenvector and the right eigenvector, respectively. The participation factor can be used to select the PSS site [22]. Figure 6 shows the participation factors of the lowest frequency mode. Generator GB1 has the largest participation factor indicating that PSS

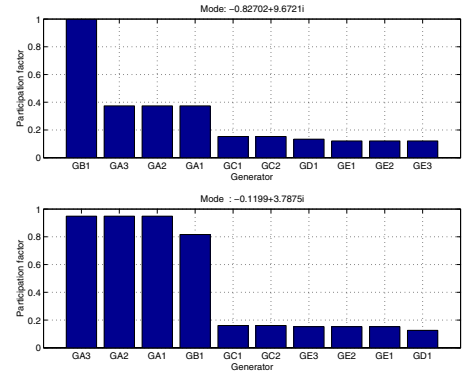


Fig. 6. Speed participation factors of the lowest frequency mode.

on Generator GB1 will yield the best damping improvement. Hence, the PSS is installed on the generator GB1.

### C. PSS Design

The above LMI formulation is used to design a PSS that damps out low-frequency oscillations. The PSS design can be separated two parts, as follows:

1) *Selecting Weighting Function*: The standard design practice in LMI design is to choose  $W_1$  as a high-gain low-pass filter to reject output disturbance, and  $W_2$  as a high-pass filter to reduce the control effort in the high-frequency range. Simultaneously ensuring robustness and minimizing the control effort generates a conflict in the nature of  $W_2$ . As recommended in [19], the weights  $W_1(s)$  and  $W_2(s)$  are chosen to have similar shapes:

$$W_1(s) = \frac{0.5 \times (99s + 11400)}{s^2 + 156s + 12504}, \quad W_2(s) = 5 \times \frac{0.5s + 1}{0.05s + 1}$$

2) *Dynamic Output Feedback*: The goal of this work is to design an PSS that will meet three specifications, concerning  $H_\infty/H_2$  performance and pole placement. Meeting these specifications can be considered to be a disturbance rejection problem, a noise rejection problem, and a damping improvement problem, respectively. An output-feedback controller is obtained by solving the linear minimization problem, as follows

- Step 1: Specify the pole placement area that the real parts of system poles are restricted to be less than -0.01, such the damping ratio of the controlled plant exceed 0.05.
- Step 2: Compute the minimum of  $H_\infty$  norm that satisfies the constraints. It is denoted as  $\gamma_{min}$ . In our design, the minimum  $H_\infty$  norm is  $\gamma_{min} = 1.05$ .
- Step 3: Obtain a series of values  $\gamma \geq \gamma_{min}$  at the prescribed upper bound of the closed-loop  $H_\infty$  norm, and solve the constrained mixed  $H_\infty/H_2$  problem to yield a series of values of  $\nu$  corresponding to the upper bound on  $H_2$  norm. Figure 7 plots the trade-off between the  $H_\infty$  and  $H_2$  performance. This curve shows that the output-feedback controller obtained at the point  $\gamma_{min} = 1.2$  gives the best compromise between the two objectives.

The multi-objective controller is obtained by using the function *hinfmix* of the *LMI control Toolbox* in Matlab [26]. The LMI-based design is such that the order of the controller in the LMI

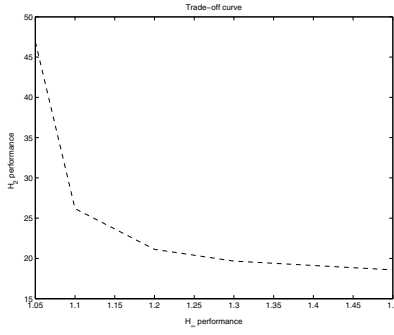


Fig. 7. Trade-off curve

solution equals to the reduced plant order plus the order of the weights. The resulting 13th-order PSS is

$$PSS_o(s) = \frac{N_o(s)}{D_o(s)}$$

where

$$\begin{aligned} N_o(s) &= -11508s^{12} - 2.231e6s^{11} + 2.123e9s^{10} - 5.009e9s^9 \\ &+ 5.469e10s^8 + 3.027e12s^7 + 4.68e13s^6 + 5.219e14s^5 \\ &+ 2.77e15s^4 + 1.368e16s^3 + 3.81e16s^2 + 3.46e16s + 8.074e15 \\ D_o(s) &= s^{13} + 454.78s^{12} + 92595s^{11} + 1.044e7s^{10} + 6.719e8s^9 \\ &+ 2.233e10s^8 + 3.336e11s^7 + 3.767e12s^6 + 2.581e13s^5 \\ &+ 1.158e14s^4 + 3.9e14s^3 + 5.84e14s^2 + 1.74e14s + 7.186e12 \end{aligned}$$

#### D. Reducing the PSS Model

The 13-th order controller is very awkward to implement practically, so the Hankel-norm reduction techniques are employed to obtain an approximate low-order controller. Figure 8 shows the magnitude of the singular values of the 13th-order controller. The figure shows that the differences between the first five and other singular values is very large. A simple 5th-order controller using the Hankel norm is recommended to approximate the original controller. Figure 9 compares the Bode responses of the original controller and the reduced controller. The Hankel norm yields good approximate results. This 5th-order controller is used to construct the PSS. The transfer function of the PSS is

$$PSS_n(s) = \frac{N(s)}{D(s)}$$

where

$$\begin{aligned} N(s) &= 5.19s^5 - 15593s^4 + 3.35e5s^3 + 1.05e6s^2 + 1.23e7s + 1.87e7 \\ D(s) &= s^5 + 352.89s^4 + 21848s^3 + 45166s^2 + 3.39e5s + 16709 \end{aligned}$$

#### E. Verifying Pole Positions

Figure 10 shows the distributions of system poles of the reduced system with and without the 5th-order PSS. As required by the design specifications, the controller provides the required damping and shift the system poles into the desired region of the complex plane. Table III reports the frequencies  $f(H_z)$  and the damping ratio  $\zeta(\%)$  for the two lowest-frequency modes. Hence, as the system equipped with the designed PSS, the damping ratio of the system exceeds the minimum requirement of  $\zeta = 0.05$ .

TABLE III  
COMPARISONS OF THE LOWEST TWO FREQUENCY MODES

Mode	without LMI PSS		with LMI PSS	
	$f(H_z)$	$\zeta(\%)$	$f(H_z)$	$\zeta(\%)$
$-0.012 \pm j3.79$	0.603	0.32	0.586	25.4
$-0.827 \pm j9.67$	1.544	8.64	1.576	18.5

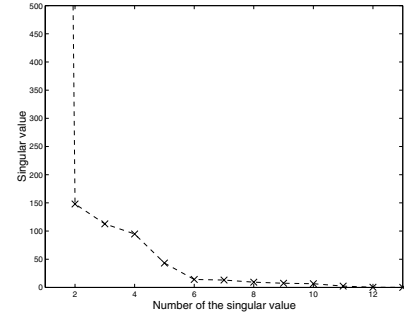


Fig. 8. Singular values of the robust PSS

#### F. Nonlinear Simulations

Nonlinear simulations are performed to evaluate the performance of the controllers under large disturbances to verify the robustness of the designed PSS. The power system transient simulation tool *PSS/E Ver 28.1* is performed. Three-phase faults are applied to one of the following tie-lines :

- 1) Case 1: The line connecting buses #1 – #2.
- 2) Case 2: The line connecting buses #2 – #3.
- 3) Case 3: The line connecting buses #2 – #5.

The fault persists for 57ms, after which the circuit was disconnected by suitable circuit breakers. Figure 11-12 show nonlinear simulation results. The conventional PSS is designed following the approach in [2]. The transfer function of the conventional PSS is

$$PSS_c(s) = \frac{26.62s^3 + 233.521s^2 + 661.157s}{s^3 + 51.587s^2 + 667.587s + 82.645}$$

From simulation results, it can be observed that the LMI PSS provides robust stability and good performance in time domain analysis. Hence, given a large disturbance, the performance of the proposed robust PSS is very favorable.

#### V. CONCLUSION

The mixed-sensitivity based on multi-objective control in the LMI framework was applied successfully to the largest industrial power system in Taiwan, which suffers from low-frequency oscillations. The pole placement constraint was appended to the  $H_\infty/H_2$  performance by designing a robust PSS. The robust PSS improves the system damping with reasonable controller orders. The robustness of the designed PSS was confirmed verified in the frequency domain by eigen-analysis. Nonlinear time domain simulations were also performed to validate the PSS design.

#### REFERENCES

- [1] V. Vittal, N. Bhatia, and A. A. Fouad, "Analysis of the inter-area mode phenomenon in power systems following large disturbance," *IEEE Trans. on Power Systems*, vol. 6, no. 4, pp. 1515–1521, Jan. 1991.
- [2] E. V. Larsen and D. A. Swann, "Applying power system stabilizers(three parts)," *IEEE Trans. on Power Systems*, vol. 100, no. 6, pp. 3017–3046, 1981.

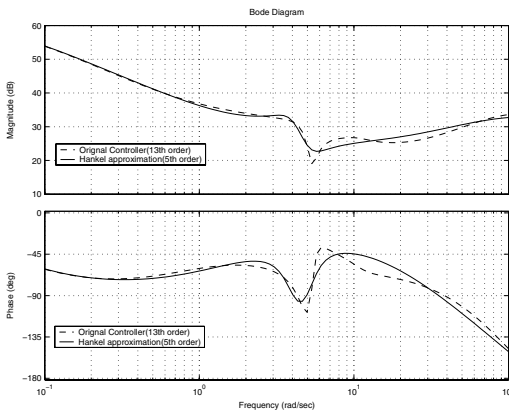


Fig. 9. Bode response of the robust PSS : the real line is 13-th order PSS. The dash line is 5-th order reduced PSS.

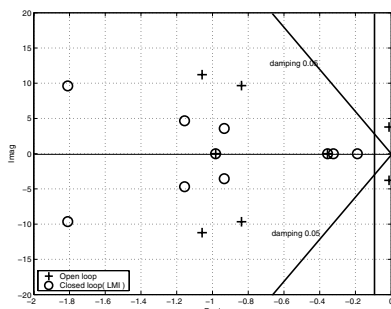


Fig. 10. System Pole Distribution Plot: + denotes the open loop pole. o denotes the closed loop pole.

- [3] M. J. Gibbard, N. Martins, J. J. Sanchez-Gasca, N. Uchida, and V. Vittal, "Recent applications of linear analysis techniques," *IEEE Trans. on Power Systems*, vol. 16, no. 1, pp. 154–162, Feb. 2001.
- [4] P. L. So and D. C. Macdonald, "Analysis and control of inter-area oscillations for system security enhancement," *IEE Power System Control and Management Conference*, pp. 65–70, 1996.
- [5] C. L. Chang, C. S. Liu, and C. K. Ko, "Experience with power system stabilizers in a longitudinal power system," *IEEE Trans. on Power Systems*, vol. 10, no. 1, pp. 539–545, Feb. 1995.
- [6] G. J. Rogers, "The application of power system stabilizers to a multi-generator plant," *IEEE Trans. on Power Systems*, vol. 15, no. 1, pp. 350–355, Feb. 2000.
- [7] Y. M. Park, M. S. Choi, J. W. Lee, and K. Y. Lee, "An auxiliary LQG/LTR robust controller design for cogeneration plants," *IEEE Trans. on Energy Conversion*, vol. 11, no. 2, pp. 407–413, Jun. 1996.
- [8] R. Asgharian, "A robust  $H_\infty$  power system stabilizer with no adverse effect on shaft torsional modes," *IEEE Trans. on Energy Conversion*, vol. 9, no. 3, pp. 475–481, Sep. 1994.
- [9] F. K. A., N. Yorino, and H. Sasaki, "Design of  $H_\infty$ -pss using numerator-denominator uncertainty representation," *IEEE Trans. on Power Systems*, vol. 12, no. 1, pp. 45–50, Mar. 1997.
- [10] M. M. Farsangi, Y. H. Song, and M. Tan, "Applying  $H_\infty$  optimization method to power system stabilizer design Part1: single-machine infinite-bus systems and Part2: multi-machine power systems," *International Journal of Electrical Power and Energy Systems*, vol. 19, no. 1, pp. 29–43, 1997.
- [11] K. A. Folly, N. Yorino, and H. Sasaki, "Improving the robustness of  $H_\infty$ -PSS using the polynomial approach," *IEEE Trans. on Power Systems*, vol. 13, no. 4, pp. 1359–1364, Nov. 1998.
- [12] M. Klein, L. X. Le, G. J. Rogers, S. Farrokhpay, and N. J. Balu, " $H_\infty$  damping controller design in large power systems," *IEEE Trans. on Power Systems*, vol. 10, no. 1, pp. 158–166, Feb. 1995.
- [13] S. Chen and O. P. Malik, "Power system stabilizer design using  $\mu$  synthesis," *IEEE Trans. on Energy Conversion*, vol. 10, no. 1, pp. 175–181, 1995.
- [14] M. Djukanovic, M. Khammash, and V. Vittal, "Application of the structured singular value theory for the robust stability and control analysis on multimachine power systems, Part1: framework development

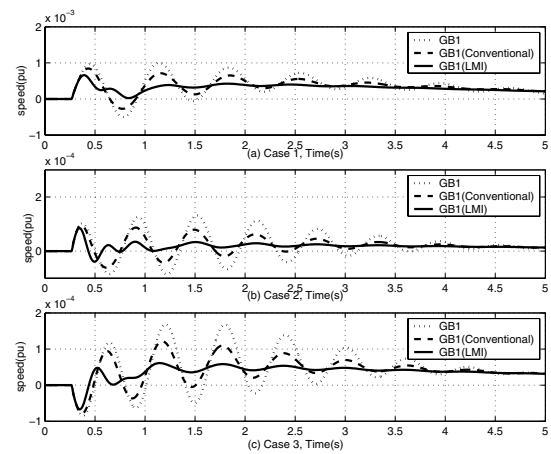


Fig. 11. Generator speed of the system following fault under the following three cases (1) GB1 with no PSS, (2) GB1(Conventional) with the conventional PSS, (3) GB1(LMI) with the robust LMI PSS.

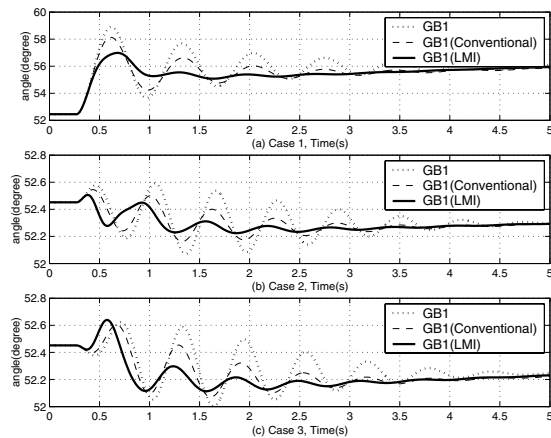


Fig. 12. Generator angle of the system following fault under three cases (1) GB1 without PSS, (2) GB1 with one conventional PSS, (3) GB1(LMI) with one LMI robust PSS.

- and Part2: numerical simulation and results," *IEEE Trans. on Energy Conversion*, vol. 13, pp. 1311–1316, 1998.
- [15] —, "Sequential synthesis of structured singular value based decentralized controllers in power systems," *IEEE Trans. on Power Systems*, vol. 14, no. 2, pp. 635–641, May. 1999.
  - [16] C. Zhu, M. Khammash, V. Vittal, and W. Qiu, "Robust power system stabilizer design using  $H_\infty$  loop shaping approach," *IEEE Trans. on Power Systems*, vol. 18, no. 2, pp. 810–818, May. 2003.
  - [17] C. Scherer, P. Gahinet, and M. Chilali, "Multiobjective output-feedback control via LMI optimization," *IEEE Trans. on Automatic Control*, vol. 42, no. 7, pp. 896–911, Jul. 1997.
  - [18] H. Werner, P. Korba, and T. C. Yang, "Robust tuning of power system stabilizers using LMI-techniques," *IEEE Trans. on Control Systems Technology*, vol. 11, no. 1, pp. 147–152, Jan. 2003.
  - [19] B. Chaudhuri, B. C. Pal, A. C. Zolotas, I. M. Jaimoukha, and T. C. Green, "Mixed-sensitivity approach to  $H_\infty$  control of power system oscillations employing multiple facts devices," *IEEE Trans. on Power Systems*, vol. 18, no. 3, pp. 1149–1156, Aug. 2003.
  - [20] P. S. Rao and I. Sen, "Robust pole placement stabilizer design using linear matrix inequalities," *IEEE Trans. on Power Systems*, vol. 15, no. 1, pp. 313–319, Feb. 2000.
  - [21] PTI, *PSS/E28 on-line Documentation*. Power Technologies Inc., 2001.
  - [22] G. Rogers, *Power System Oscillations*. Kluwer Academic, 2000.
  - [23] P. Kundur, *Power System Stability and Control*. McGraw-Hill, 1994.
  - [24] A. Nemirovski and P. Gahinet, "The projective method for solving linear matrix inequalities," *Amer. Contr. Conf.*, pp. 840–844, 1994.
  - [25] G. J. Balas, J. C. Doyle, and et al,  *$\mu$ -Analysis and Synthesis Toolbox for Use With MatLab*. The Math Works Inc, 2001.
  - [26] P. Gahinet, A. Nemirovski, A. J. Laub, and M. Chilali, *LMI Control Toolbox for Use With MatLab*. The Math Works Inc, 1995.